Original Article

Three-dimensional spheroids of dedifferentiated fat cells enhance bone regeneration

Tsukasa Yanagi [a, b], Hiroshi Kajiya [a, c, *], Seiichi Fujisaki [a, b], Munehisa Maeshiba [a, b], Ayako Yanagi-S [b], Nana Yamamoto-M [d], Kae Kakura [b], Hirofumi Kido [b], Jun Ohno [a]

[a] Oral Medicine Research Center, Fukuoka Dental College, 2-15-1Tamura, Fukuoka, Japan
[b] Department of Oral Rehabilitation, Fukuoka Dental College, 2-15-1Tamura, Fukuoka, Japan
[c] Department of Physiological Science and Molecular Biology, Fukuoka Dental College, 2-15-1Tamura, Fukuoka, Japan
[d] Department of Odontology, Fukuoka Dental College, 2-15-1Tamura, Fukuoka, Japan

A B S T R A C T

Introduction: Mesenchymal stromal/stem cells (MSCs) are multipotent, self-renewing cells that are extensively used in tissue engineering. Dedifferentiated fat (DFAT) cells are derived from adipose tissues and are similar to MSCs. Three-dimensional (3D) spheroid cultures comprising MSCs mimic the biological microenvironment more accurately than two-dimensional cultures; however, it remains unclear whether DFAT cells in 3D spheroids possess high osteogenerative ability. Furthermore, it is unclear whether DFAT cells from 3D spheroids transplanted into calvarial bone defects are as effective as those from two-dimensional (2D) monolayers in promoting bone regeneration.
Methods: We compared the in vitro osteogenic potential of rat DFAT cells cultured under osteogenic conditions in 3D spheroids with that in 2D monolayers. Furthermore, to elucidate the ability of 3D spheroid DFAT cells to promote bone healing, we examined the in vivo osteogenic potential of transplanting DFAT cells from 3D spheroids or 2D monolayers into a rat calvarial defect model.
Results: Osteoblast differentiation stimulated by bone morphogenetic protein-2 (BMP-2) or osteogenesis-inducing medium upregulated osteogenesis-related molecules in 3D spheroid DFAT cells compared with 2D monolayer DFAT cells. BMP-2 activated phosphorylation in the canonical Smad 1/5 pathways in 3D spheroid DFAT cells but phosphorylated ERK1/2 and Smad2 in 2D monolayer DFAT cells. Regardless of osteogenic stimulation, the transplantation of 3D DFAT spheroid cells into rat calvarial defects promoted new bone formation at a greater extent than that of 2D DFAT cells.
Conclusions: Compared with 2D DFAT cells, 3D DFAT spheroid cells promote osteoblast differentiation and new bone formation via canonical Smad 1/5 signaling pathways. These results indicate that transplantation of DFAT cells from 3D spheroids, but not 2D monolayers, accelerates bone healing.
© 2021, The Japanese Society for Regenerative Medicine. Production and hosting by Elsevier B.V. This is an open access article under the CC BY-NC-ND license (http://creativecommons.org/licenses/by-nc-nd/4.0/).

1. Introduction

Mesenchymal stem/stromal cells (MSCs) are multipotent somatic stem cells that can differentiate into various mesodermal cells such as osteoblasts, chondrocytes, myocytes, and adipocytes [1]. MSCs offer unique opportunities for cellular therapy because of their ability to stimulate the regeneration of damaged tissues and organs [2,3]. Adipose tissues are abundant throughout the body and are known to contain two types of stem/stromal cells, namely, adipose-tissue-derived MSCs (ASCs) and dedifferentiated fat (DFAT) cells [4,5]. DFAT cells make a highly homogeneous and proliferative cell population and possess multilineage potential for differentiation into mesenchymal tissue lineages under suitable culture conditions [6,7].

Two-dimensional (2D) monolayers are standard in traditional in vitro cell culture. However, these conditions have been reported to adversely affect self-renewal, replication, colony-forming efficiency, and differentiation capacity [8,9]. In contrast,

three-dimensional (3D) spheroid cultures are considered physiologically more similar to *in vivo* conditions; therefore, the above-mentioned behaviors are better preserved when using 3D spheroid cultures [10–12]. We recently reported that mouse MSCs from 3D spheroids promote osteogenesis and bone healing via Wnt/beta-catenin activation at a greater extent than MSCs from 2D monolayers [13]. However, whether osteogenesis is promoted at a greater extent by DFAT cells grown in 3D spheroids or those in 2D monolayers remains unclear. Furthermore, it is unclear whether differences in the two culture conditions affect bone regeneration in response to the transplantation of DFAT cells into bone defects.

In the present study, we assessed whether the osteogenerative potential of 3D-spheroid DFAT cells is greater than that of 2D monolayer DFAT cells *in vitro*. In addition, to elucidate the ability of 3D MSCs to regenerate bone, we examined the effects of 2D-monolayer and 3D-spheroid DFAT cells on new bone formation in a rat calvarial defect model *in vivo*.

2. Experimental methods

2.1. Isolation and ceiling culture of DFAT cells

All animals were used in accordance with the National Institute of Health guidelines and the protocols approved by the Animal Care Committee of the Fukuoka Dental College, Fukuoka, Japan (Certification Nos. 17004 and 18004).

We isolated DFAT cells from abdominal adipose tissue following the protocol reported in a previous report [14]. In brief, approximately 1 g of abdominal adipose tissue was collected from a male rat (24–30-week-old, Kyudo Co., Tosu, Japan). The tissue was minced into fine pieces and digested with 0.1% collagenase solution (Collagenase Type I, Koken Co., Ltd., Tokyo, Japan) and was incubated in a container at 37 °C for 1 h. After filtration and low-speed centrifugation at 1400 rpm for 1 min, the floating layer at the top that contained the isolated adipocytes was collected. Approximately three drops of mature adipocytes were dropped into a flask containing Dulbecco's Modified Eagle's Medium (DMEM, Fuji Film Wako, Japan) with 20% fetal bovine serum (FBS, Sigma–Aldrich Co., St. Louis, MO, USA). The cells floated and attached to the top of the flask. After 7 days, the medium was removed and the flask was turned upside down so that the cells were at the bottom. After allowing the adherent cells to grow to approximately 80% confluence, they were either replated into monolayer cultures or used to form spheroids. DFAT cells were used for experiments before they reached the fifth passage. DFAT cells were used to generate spheroids based on the protocol described by Itaka et al. [15]. The cells (4×10^5 cells/ml) were added to Cell able® low cell-binding surface 24-well plates (Toyo Gosei, Tokyo, Japan) and incubated in DMEM at 37 °C for up to 48 h. After replating the 3D spheroid DFAT cells in culture dishes, they were cultured in DMEM supplemented with 10% FBS. In some experiments, the 2D monolayer or 3D spheroid DFAT cells were cultured in DMEM with bone morphogenetic protein-2 (BMP-2) (30 ng/ml, Pepro Tech. Inc., NJ, USA) or osteogenesis-inducing medium (OIM) with β-glycerophosphate (10 mM, Sigma) and ascorbic acid (50 μg/mL, Sigma). In some experiments, the DFAT cells were cultured with BMP-2 in the presence or absence of ERK1/2 inhibitor (U0126, Merck Co. Ltd.).

2.2. RNA isolation and quantitative reverse transcription polymerase chain reaction

Total RNA was extracted from cells using TRIzol reagent. First-strand complementary DNA (cDNA) was synthesized from 3 μg total RNA using SuperScript II reverse transcriptase according to the manufacturer's instructions (Invitrogen Carlsbad, CA, USA). To detect mRNA expression, we selected specific primers based on the nucleotide sequence of the resultant cDNA (Table 1). Relative mRNA expression was normalized as the ratio of targeted mRNAs to β-actin expression levels. All reactions were executed in hexaplicate.

2.3. Western blot analyses

Cells were lysed in the TNT (0.1M Tris.HCl, pH 7.5; 0.15M NaCl; 0.05% Tween-20; Roche, Basel, Switzerland) buffer. Protein content was measured using a protein assay kit (Pierce, Hercules, CA, USA). Of each protein, 20 μg were subjected to 10.0% sodium dodecyl sulfate polyacrylamide gel electrophoresis, and the separated proteins were electrophoretically transferred to a polyvinylidene fluoride membrane at 100 V and 4 °C for 1.5 h. The membrane was incubated with antibodies against alkaline phosphatase (ALP; Abcam Co. Ltd, Cambridge, England; Cat. No. ab108337), Runx2 (Cell Signaling Technology [CST], Tokyo, Japan; Cat. No. ab22552), Osterix (Abcam; Cat. No. ab22552), p-Smad1/5 (CST; Cat. No. #13820), p-Smad2 (CST; Cat. No. #3108), p-ERK1/2 (CST; Cat. No. #4370), Smad1 (CST Cat. No. #6944), Smad2/3 (CST; Cat. No. #8685), ERK1/2 (CST; Cat. No. #4695), and β-actin (Sigma–Aldrich Co., Tokyo, Japan; Cat. No. A5441) diluted 1:500 in tris-buffered saline with tween (TBST: 10 mM tris–HCl, 50 mM NaCl, 0.25% Tween-20) plus 0.01% azide and 5% skim milk overnight at 4 °C. The blots were washed in TBST and incubated for 1 h with horseradish peroxidase-conjugated antirabbit or antimouse immunoglobulin-G secondary antibodies. The antibodies were diluted (1:2000) in 5% skim milk TBST and were developed using an enhanced chemiluminescent system (GE Healthcare, Tokyo, Japan).

2.4. Flow cytometry analyses

Fluorescence-activated cell sorting (FACS) was performed to characterize the DFAT cells. The following antibodies conjugated with fluorescein isothiocyanate (FITC) or phycoerythrin (PE) were used as MSC markers: anti-CD29-PE, anti-CD44-FITC, anti-CD90-PE, and mouse IgGa1 isotype control (BD Bioscience, CA, USA). The labeled cells were analyzed through flow cytometry using the On-chip system (On-chip Biotechnologies Co., Ltd., Tokyo, Japan). The ratio of each antibody-positive cell to the total cells was quantified using the associated analysis software.

2.5. Alizarin red staining

After culturing with or without OIM, the cells were washed twice with PBS and fixed in 4% paraformaldehyde for 10 min. The cells were then stained with 1% alizarin red solution for 5 min. To quantify alizarin red staining, the stained cells were lysed in 5% formic acid at room temperature for 10 min. The cell lysates were then collected and were quantified at an absorbance wavelength of 450 nm using a plate reader (ARVO MX, PerkinElmer, MA, USA).

2.6. Transplantation of cells into a rat model of calvarial bone defects

All surgeries were performed under general anesthesia induced by 2% isoflurane (Abbott Laboratories, Abbort Park, IL, USA) using an air–gas mixing machine (Anesthesia machine SF-B01; MR Technology, Inc., Tsukuba, Ibaraki, Japan). All efforts were made to minimize animal suffering. A circular bone defect (full-thickness, 8 mm diameter) was created in the calvarial bone with a trephine drill and irrigated with saline to remove any bone debris. Controls for the transplant experiments included calvarial defects transplanted with an absorbable collagen sponge (CS; Zimmer Biomet Holdings, Inc., Warsaw, USA) of the type used as a wound dressing

Table 1
Quantitative RT-PCR primers.

Genes	Forward and reverse primers (5′-3′)	position	Product size (bp)	Acc No
ALP	5′-ACGAGGTCACGTCCATCCT	586–604	71	NM_013059
	5′-CCGAGTGGTGGTCACGAT	656–639		
Runx2	5′-GGCCCTGGTGTTTAAATGG	75–93	54	NM_001278483
	5′-AGCACTCACTGACTCGGTTG	147–128		
OSX	5′-CCCAACTGTCAGGAGCTAGA	808–827	61	NM_001037632
	5′-GATGTGGCCGGCTGTGAAT	885–868		
β-actin	5′-CCCGCGAGTACAACCTTCT	20–38	69	NM_031144
	5′-CGTCATCCATGGCGAACT	88–71		

in dental surgery. The rats were divided into five groups: a) the control group with 8 mm CSs in the bone defects (n = 5), b) the 2D monolayer DFAT cell transplantation group (n = 5), c) the osteogenic 2D monolayer DFAT cell transplantation group in which osteogenesis had been induced by incubation with OIM for 7 days (n = 5), d) the 3D spheroid DFAT cell transplantation group (n = 5), and e) the 3D spheroid DFAT cell transplantation group in which osteogenesis had been induced (n = 5).

2.7. Microcomputer tomography analyses

Microcomputed tomography (μ-CT) images (Skyscan-1176, Bruker, Belgium) were obtained *in vivo* at 50 kV and 500 mA. Each μ-CT slice had a thickness of 35 μm. The percentage of new bone formation in the bone defect was calculated from each μ-CT image as the area of the newly formed bone relative to the area of the original defect as described in our previous report [16]. First, the areas of newly formed bone in sagittal μ-CT images were quantified in two dimensions using WINROOF (Mitani Corporation, Tokyo, Japan). On each μ-CT image, 8-mm circles were drawn for analysis. A series of 10 μ-CT images that showed the areas with the highest amounts of new bone formation were used for the analysis of each sample. The percentage of new bone formation in the defect (% of new bone) was calculated as the total area of new bone formed in five μ-CT images, × 100. Before measurements, images were adjusted so that the top of calvaria was positioned in the vertical plane. Edited images were stored and analyzed using CT-An image analysis software (Bruker, Belgium). The 30 sections with the calvaria bone were used and analyzed to measure the bone mineral density (BMD) used in bone surgical regions after transplantation in a rat model of calvarial bone defects.

2.8. Hematoxylin and eosin staining

Rat calvarial bone was collected at 12 weeks after transplantation. The samples were fixed in 4% (w/v) paraformaldehyde/phosphate buffer (pH 7.4), decalcified with 0.24 M ethylenediamine tetra-acetic acid solution, dehydrated with a graded alcohol series, cleared in xylene, and embedded in paraffin. Staining was performed using 3 μm-thick sections following standard protocols. The paraffin-embedded sections were stained with hematoxylin and eosin (HE) and toluidine blue to evaluate any histological changes. The border line between the newly formed bones and old bones were evaluated based on the difference in the staining intensity of eosin. All sections were histologically observed with a Nikon Eclipse fluorescence microscope (Nikon, Tokyo, Japan).

2.9. Statistical analyses

Data are expressed as mean ± standard error of the mean. Differences were analyzed using one-way analysis of variance and Scheffe's multiple comparisons test. P-values of <0.05 were considered significant.

3. Results

3.1. Osteogenic stimulation significantly upregulated osteogenesis-related molecules in DFAT cells

To characterize DFAT cells as stem/stromal-like cells, FACS was first performed using the cells collected from the adipose tissues. Almost all DFAT cells (>85%) were positive for mesenchymal stem markers (CD44, CD90, and CD29; Fig. 1A).

We examined morphological changes in cultured 2D monolayer and 3D spheroid DFAT cells. Although both types of DFAT cells proliferated and spread in a time-dependent manner, there remained a small number of spheroids even through day 7 in culture (Fig. 1B). Furthermore, no cytological changes such as apoptosis or necrosis were observed in either 2D monolayer or 3D spheroid DFAT cells. To assess the differences in calcium secretion between 2D monolayer and 3D spheroid DFAT cells, both types of cells were cultured with OIM. Alizarin red staining increased on day 14 after the induction of osteogenesis in 2D monolayers and on day 7 in 3D spheroids (Fig. 1C). Furthermore, the extent of alizarin red staining was higher in 3D DFAT cells than in 2D culture on days 14 and 21 after the induction of osteogenesis.

Treatment with BMP-2 (30 ng/mL) increased the expression of mRNA from osteogenesis-related genes such as ALP (Alpl), Runx2 (Runx2), and OSX (Sp7), compared with those in the control (without BMP-2) in both 2D and 3D cell culture (data not shown). Furthermore, after BMP-2 treatment, the expression of these mRNAs was significantly more upregulated in 3D DFAT cells in a time-dependent manner than in 2D DFAT cells (Fig. 2A). Although ALP, Runx2, and OSX mRNA expression in response to BMP-2 treatment increased by day 3 in both types of DFAT cells, the increase was greater in 3D than in 2D DFAT cells. Similar results were obtained after the cells were stimulated with OIM.

Consistent with the increased mRNA levels, osteogenic stimulation by BMP-2 upregulated osteogenesis-related proteins such as ALP, Runx2, and OSX in a dominant and time-dependent manner that was more marked in 3D than in 2D DFAT cells (Fig. 2B). The data indicated that the 3D DFAT cells were stimulated more than the 2D cells toward osteoblast differentiation.

Furthermore, BMP-2 mainly activated the expression and phosphorylation of ERK1/2 and Smad2 in 2D-monolayer DFAT cells. In 3D DFAT cells, however, BMP-2 mainly phosphorylated Smad1/5 but not Smad2 and there was a greater reduction in total Smad1/5 protein levels in the 3D DFAT cells than in the 2D DFAT cells during osteogenesis (Fig. 2C). The phosphorylation of ERK1/2 also increased at a greater extent in 3D than in 2D DFAT cells.

To clarify whether an upstream enzyme ERK1/2 activation further promotes osteogenesis in 2D DFAT cells, little 3D DFAT cells, we examined the effects of U0126, an ERK1/2 inhibitor (Fig. 2D), on
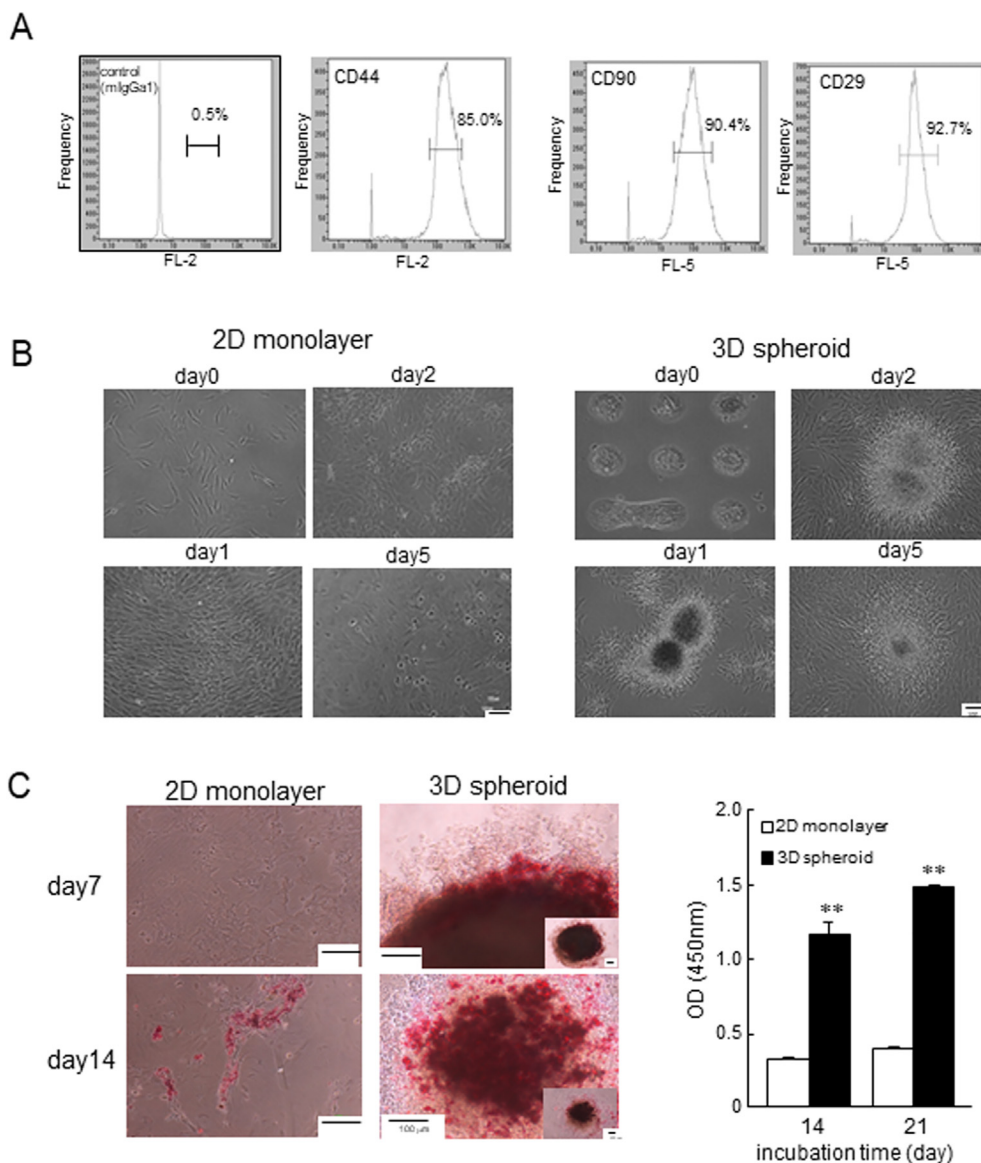
Fig. 1. Flow cytometric analysis and representative images of cultured and alizarin red—stained 2D monolayer and 3D spheroid dedifferentiated fat (DFAT) cells. (A) Ratio of positive cells in CD44, CD29, and CD90 stemness markers in DFAT cells. Mouse IgGa1was used as the control. (B) Phase contrast images of cultured 2D monolayer and 3D spheroid DFAT cells. Scale bar = 100 μm. (C) Alizarin red staining showed calcium deposition in OIM-treated 2D monolayer and 3D spheroid DFAT cells. Scale bar = 100 μm. Calcium deposition rates were calculated at 14 and 21 weeks in alizarin red staining after OIM stimulation. Data shown are the means from three wells (mean ± standard error of the mean). Symbol ** denotes p < 0.01 in 2D vs. 3D DFAT cells.

the expression of osteogenesis-related molecules in the present study. BMP-2 incubation with U0126 dramatically suppressed the expression of osteogenesis-related genes in 2D DFAT cells but partially suppressed the expression in 3D DFAT cells, suggesting that the expression of BMP-2-induced genes was activated in 2D DFAT cells, but less in 3D DFAT cells, through the ERK1/2-Smad2/3 signaling pathway.

3.2. Transplantation with 3D DFAT cells significantly promoted new bone formation in a rat model of calvarial bone defects

To clarify whether the promotion of new bone formation occurs at a higher rate in 3D DFAT cells than in 2D DFAT cells, we transplanted a CS scaffold (control) or 2D/3D DFAT cells into rats with a calvarial bone defect (Fig. 3A and B). In parallel experiments, both types of DFAT cells were transplanted after osteogenic stimulation for 7 days. After 2 weeks from transplantation, μ-CT images

revealed no differences in the rat calvarial bone defects among the control animals and those transplanted with 2D or 3D DFAT cells. After 12 weeks from transplantation, new bone formed around the defects in rats transplanted with 2D or 3D DFAT cells at rates higher than those in the control groups. Furthermore, osteogenic stimulation of 2D and 3D DFAT cells before transplantation promoted the formation of new calvarial bone beyond that observed with unstimulated cells. Bone formation was stimulated to a greater extent by 3D than by 2D DFAT cells whether or not they had experienced osteogenic stimulation. Consistent with the μ-CT data, histological analysis of HE-stained sections and toluidine blue-stained showed that new bone regeneration at 12 weeks after the transplantation was significantly greater in rats transplanted with 3D DFAT cells than in the control rats or those transplanted with 2D DFAT cells (Fig. 3C). The transplantation of either 2D or 3D DFAT cells that had experienced osteogenic stimulation increased the formation of new calvarial bone slightly more than the transplantation of
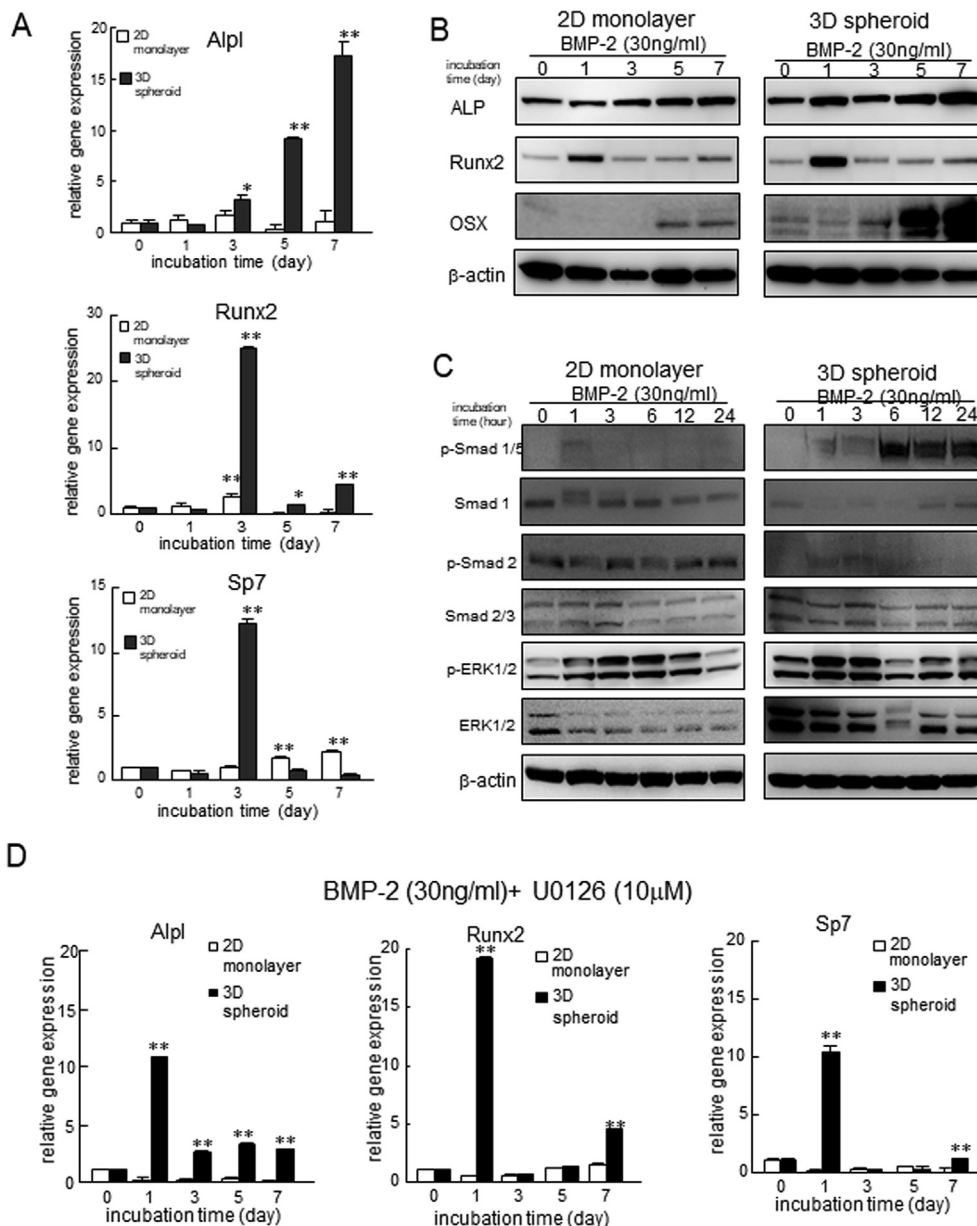
Fig. 2. **Effects of BMP-2 stimulation on the expression of osteogenesis-related molecules in 2D monolayer and 3D spheroid DFAT cells**. (A) DFAT cells in 2D and 3D cultures were treated with BMP-2 (30 ng/mL). Expression of the osteogenesis-related genes Alpl (ALP), Runx2, and Sp7 (Osterix) increased in cells from both types of cultures following incubation with BMP-2. Samples were analyzed by quantitative reverse transcription polymerase chain reaction and were normalized to β-actin mRNA. Data shown are the means from six culture wells (mean ± standard error of the mean). Symbols * and **, respectively, indicate $p < 0.05$ and $p < 0.01$ in 2D vs. 3D DFAT cells. (B) 2D and 3D DFAT cells were treated with BMP-2 (30 ng/mL). Western blotting was performed using targeted and β-actin antibodies in 2D and 3D DFAT cells. Similar results were obtained in three independent experiments. (C) DFAT cells were treated with BMP-2 (20 ng/mL). The expression of BMP receptor downstream the signaling molecules such as ERK1/2, Smad1/5, and Smad2/3 and their phosphorylated proteins following BMP-2 incubation. Samples were analyzed using Western blot analysis and normalized to β-actin proteins. Similar results were obtained in four independent experiments. (D) Two- and three-dimensional DFAT cells were treated with BMP-2 in the presence or absence of U106 (10 μM), an ERK1/2 inhibitor. The expression of osteogenesis-related genes in DFAT cells following BMP-2 (20 ng/mL) incubation. Samples were analyzed using quantitative reverse transcription polymerase chain reaction and normalized to β-actin mRNA. Data shown are the means from five culture wells (mean ± standard error of the mean). Symbols ** indicates $p < 0.01$ in 2D monolayer vs. 3D spheroid DFAT cells.

unstimulated cells. Furthermore, toluidine blue staining results revealed that the newly formed areas comprised layered bone in the lateral side and sponged-like bone in the medial side. The new bone area in 3D DFAT transplantation was higher calcification than that of 2D DFAT.

BMD increased in the surgical site of the transplantation of 3D DFAT cells compared with that of the transplantation of 2D DFAT cells at 12 weeks after the transplantation (Fig. 3D). Furthermore, the BMD in osteogenic stimulation of 3D DFAT cells before transplantation significantly increased compared with the control.

However, no significant difference was noted in the BMD of 3D DFAT transplantation with or without osteogenic stimulation at 12 weeks after the surgery, suggesting that the bone in surgical regions may be incomplete calcification.

4. Discussion

The 3D cultures of MSCs have been reported to allow the cells to adapt to their native shape, upregulate cell-to-cell contacts, and interact with the extracellular matrix [15,17]. In the present
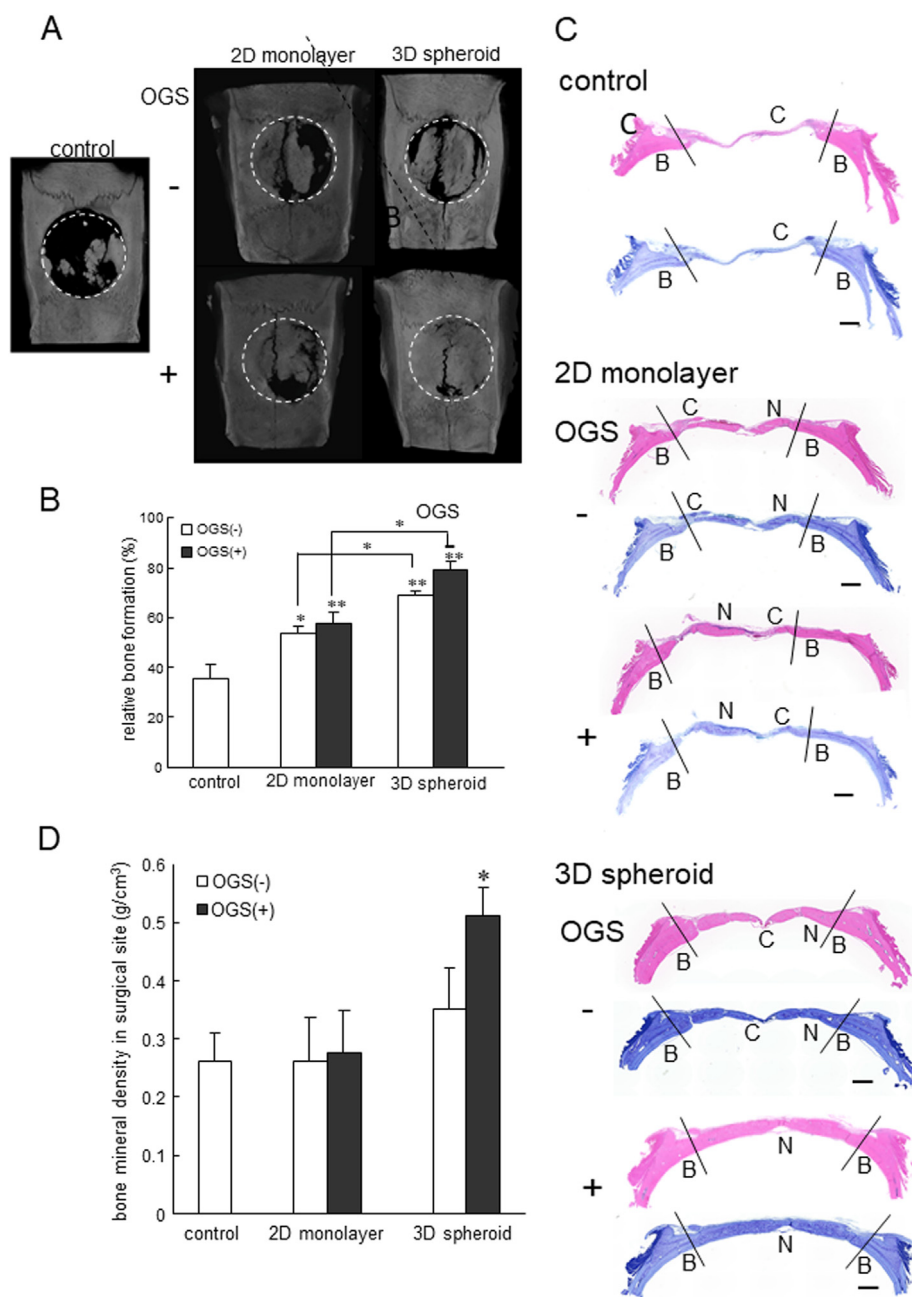
Fig. 3. Transplantation with 3D spheroid DFAT cells promoted new calvarial bone formation in rats. (A) Vertical microcomputed tomography (μ-CT) images of bone defects in rats (age: 10 weeks) transplanted with cells from both 2D and 3D cultures. The images on the left show cases where a CS scaffold (control) was transplanted, the central images show cases where CS scaffolds containing 2D DFAT cells were transplanted, and the images on the right show CS scaffolds containing 3D DFAT cells with or without prior osteogenesis stimulation (OGS) with osteogenesis-inducing medium for 7 days. The white dashed circles indicate calvarial bone defects (8 mm in diameter). (B) Calculated new bone deposition rates at 12 weeks after transplantation with or without OGS. The percentage of new bone mineral deposition was calculated from the bony tissue within the white dashed circles in the five types of grafts. Data shown are from five rats (mean ± standard error of the mean). Symbol * denotes p < 0.05, and ** denotes p < 0.01 in the control vs. each transplantation group and in 3D vs. 2D DFAT cells at 12 weeks. (C) Histological images of the sagittal sections of calvarial bone tissues at 12 weeks after transplantation. Symbols B, N, and C indicate original, new bone, and connective tissues, respectively. Scale bar = 1 mm. (D) Bone mineral density (BMD) was calculated in the surgical regions (white dashed circles) at 12 weeks after each transplantation. Data shown are the means from five rats (mean ± standard error of the mean). Symbol * denotes p < 0.05 in control vs. each transplantation group in DFAT cells at 12 weeks.

experiments, we provide evidence to support the hypothesis that 3D spheroid DFAT cells enhance osteogenic potential and promote bone regeneration more than 2D monolayer DFAT cells: the expression of osteogenesis-related molecules was upregulated in 3D spheroid DFAT cells and new bone formation was promoted after transplanting 3D spheroid MSCs into a rat model of calvarial bone defects. The transplantation of osteoinduced 3D spheroid

DFAT cells further increased new bone formation in rat calvarial bone defects.

DFAT cells have been reported to have a higher osteogenesis potential than ASCs after transplantation into a young rat model of calvarial bone defects [18,19]. In the present study, transplantation with only CSs resulted in large increases in the connective tissue but less new bone in defect areas, as noted in histological analysis.

In our study, we observed significantly greater bone regeneration following the transplantation of 3D spheroid or 2D monolayer DFAT cells using the rat model of calvarial bone defects. Functional repair of the calvarial bone requires an optimal biochemical response, and on the basis of the data obtained from alizarin staining, 3D spheroid DFAT cells possessed a greater capacity to deposit calcium than 2D monolayer DFAT cells. Furthermore, BMP-2 and OIM upregulated osteogenesis-associated molecules more in 3D spheroid DFAT cells than in 2D monolayer DFAT cells. These results suggest that the osteogenic potential of 3D spheroid DFAT cells is higher than that of 2D monolayer DFAT cells.

MSCs have been reported to generate various secretomes during 3D spheroid MSC culture, such as angiogenic cytokines and proteins associated with increased wound-healing [8,20]. Furthermore, MSCs must be primed with proinflammatory cytokines to acquire their anti-inflammatory properties [21,22], and 3D spheroid MSCs are self-stimulated by autocrine interleukin-1 signaling to have enhanced anti-inflammatory properties [23]. Furthermore, DFAT cells have also been reported to secrete several cytokines associated with bone formation and angiogenesis [24].

Transplanted green fluorescent protein–labeled DFAT cells have been observed at the transplant sites in the areas of newly formed bones [19,24]. The transplanted DFAT cells were detected at the injection site 5 weeks after transplantation. In the present study, 3D spheroid DFAT cells showed greater *in vivo* potential for calvarial bone regeneration than 2D monolayer DFAT cells at 8 weeks after the transplantation regardless of osteogenic stimulation. The findings suggest that some DFAT cells were at least partially grafted onto the transplanted calvarial bone and contributed to osteogenesis directly via the differentiation into osteoblasts and/or indirectly via the secretion of osteogenic cytokines.

A previous study used 2D monolayer DFAT cells cultured with OIM before transplantation into mandibular lesions [25]. Following the transplantation of the cells, they observed a small amount of cementum on exposed root surfaces in the lesions as well as in periodontal ligaments and soft tissues. In the present study, we found that the transplantation of osteoinduced DFAT cells stimulated thicker calvarial bone formation and higher BMD at the surgical site than nonosteoinduced or 2D DFAT cells. These findings suggest that DFAT cells are a promising source of osteoblasts for calvarial bone regeneration.

The various TGF-β superfamilies, including BMP-2, are well known to lead ligand-specific modulation of downstream signaling at all cellular levels such as the Smad1/5/8 and Smad2/3 complexes [26]. The BMP receptor has mainly been known to activate Smad1/5/9 phosphorylation in canonical downstream pathways that converge at the Runx2 gene [27,28]. Furthermore, Runx2 transcriptional activity has also been reported to be regulated by ERK-dependent phosphorylation [29]. In the present study, we found that BMP-2 phosphorylated Smad1/5 and ERK in 3D DFAT cells but only Smad2 in 2D DFAT cells. The ERK/MAPK pathway has been reported to control the differentiation of osteoblast progenitors and MSCs in response to changes in the levels of hormones, cytokines, and morphological proteins [30]. Therefore, the ERK–Smad1/5 pathway in 3D DFAT cells activated the promotion of osteoblast differentiation via the transcriptional activation of Runx2 in 3D DFAT cells.

Furthermore, the cell shape in the culture was regulated to activate downstream signaling pathway during osteogenesis in present study. One possibility is that cell aggregation in 3D spheroid is a natural shape observed into the body but 2D monolayer cells is an artificial shape, resulting in different downstream signaling between canonical pathway in Smad 1/5 in 3D DFAT cells and noncanonical pathway in Smad 2/3 in 2D DFAT cells.

Autograft transplantation suffers from an insufficient supply of donor material and significant morbidity at the donor tissue site [31]. Allografts and xenografts have inherent risks such as immunogenic response and transmission of disease from donor to recipient. Furthermore, synthetic bone scaffolds used in bone tissue engineering have usually induced insufficient osteogenesis [32]. Cytotherapy, however, has been expected to provide synergistic effects on cell differentiation and cytokine secretion from transplanted cells. Therefore, 3D DFAT cells, which were grown in a more natural biological microenvironment, are suggested to be more suitable as cell sources for cytotherapy. Combining 3D spheroid DFAT cells, particularly in the presence of osteogenesis induction, and scaffolds made from bone biomaterials would offer all these advantages and provide for more effective dental cytotherapy.

5. Conclusions

3D DFAT spheroid cells promote more osteoblast differentiation and new bone formation via canonical Smad 1/5 signaling pathways than 2D DFAT cells.

Author contributions

TY: performed experiments and generated the data.
HK: conceived and designed the study, conducted experiments, and wrote the manuscript.
SF: performed experiments and generated the data.
MM: performed experiments and generated the data.
AYS: performed experiments and generated the data.
NYM: performed experiments and generated the data.
KK: conducted experiments and analyzed the data.
HK: designed experiments and supervised the study.
JO: designed experiments and supervised the study.
All authors have read and approved the final manuscript.

Ethics approval

Approval for the animal experiments was obtained from the Animal Care Committee of Fukuoka Dental College (protocol numbers: 17004 and 18004).

Declaration of competing interest

The authors declare that they have no competing interests.

Acknowledgments

References

[1] Aldahmash A, Zaher W, May Al-Nbaheen, Kassem M. Human stromal (mesenchymal) stem cells: basic biology and current clinical use for tissue regeneration. Ann Saudi Med 2012;32:68–77.
[2] Barry FP, Murphy JM. Mesenchymal stem cells: clinical applications and biological characterization. Int J Biochem Cell Biol 2004;36:568–84.

[3] Zhang ZY, Teoh SH, Hui JHP, Fisk NM, Choolani M, Chan JKY. The potential of human fetal mesenchymal stem cells for off-the-shelf bone tissue engineering application. Biomaterials 2012;33:2656—72.

[4] Yagi K, Kondo D, Okazaki Y, Kano K. A novel preadipocyte cell line established from mouse adult mature adipocytes. Biochem Biophys Res Commun 2004;321:967—74.

[5] Kishimoto N, Honda Y, Momota Y, Tran SD. Dedifferentiated Fat (DFAT) cells: a cell source for oral and maxillofacial tissue engineering. Oral Dis 2018;24: 1161—7.

[6] Matsumoto T, Kano K, Kondo D, Fukuda N, Iribe Y, Tanaka N, et al. Mature adipocyte-derived dedifferentiated fat cells exhibit multilineage potential. J Cell Physiol 2008;215:210—22.

[7] Sakuma T, Matsumoto T, Kano K, Fukuda N, Obinata D, Yamaguchi K, et al. Mature, adipocyte derived, dedifferentiated fat cells can differentiate into smooth muscle-like cells and contribute to bladder tissue regeneration. J Urol 2009;182:355—65.

[8] Baraniak PR, McDevitt TC. Scaffold-free culture of mesenchymal stem cell spheroids in suspension preserves multilineage potential. Cell Tissue Res 2012;347:701—11.

[9] Huang GS, Tseng CS, Yen LB, Dai LG, Hsieh PS, Hsu S-h. Solid freeform-fabricated scaffolds designed to carry multicellular mesenchymal stem cell spheroids for cartilage regeneration. Eur Cell Mater 2013;26:179—94.

[10] Cesarz Z, Tamama K. Spheroid culture of mesenchymal stem cells. Stem Cell Int 2016;2016:9176357.

[11] Ader M, Tanaka EM. Modeling human development in 3D culture. Curr Opin Cell Biol 2014;31:23—8.

[12] Yin X, Mead BE, Safaee H, Robert Langer, Karp JM, Levy O. Engineering stem cell organoids. Cell Stem Cell 2016;18:25—38.

[13] Imamura A, Kajiya H, Fujisaki S, Maeshiba M, Yanagi T, Kojima H, et al. Three-dimensional spheroids of mesenchymal stem/stromal cells promote osteo-genesis by activating stemness and Wnt/β-catenin. Biochem Biophys Res Commun 2020;523:458—64.

[14] Ohta Y, Takenaga M, Tokura Y, Hamaguchi A, Matsumoto T, kano K, et al. Mature adipocyte-derived cells, dedifferentiated fat cells (DFAT), promoted functional recovery from spinal cord injury-induced motor dysfunction in rats. Cell Transplant 2008;17:877—86.

[15] Wang W, Itaka K, Ohba S, Nishiyama N, Chung UI, Yamasaki Y, et al. 3D spheroid culture system on micropatterned substrates for improved differ-entiation efficiency of multipotent mesenchymal stem cells. Biomaterials 2009;30:2705—15.

[16] Katsumata Y, Kajiya H, Okabe K, Fukushima T, Ikebe T. A salmon DNA scaffold promotes osteogenesis through activation of sodium-dependent phosphate cotransporters. Biochem Biophys Res Commun 2015;468:622—8.

[17] Kapur SK, Wang X, Shang H, Yun S, Li X, Feng G, et al. Human adipose stem cells maintain proliferative, synthetic and multipotential properties when suspension cultured as self-assembling spheroids. Biofabrication 2012;4: 025004.

[18] Suzuki D, Akita D, Tsurumachi N, Kano K, Yamanaka K, Kaneko T, et al. Transplantation of mature adipocyte-derived dedifferentiated fat cells into three-wall defects in the rat periodontium induces tissue regeneration. J Oral Sci 2017;59:611—20.

[19] Akita D, Kano K, Tamura YS, Mashimo T, Sato-Shionome M, Tsurumachi N, et al. Use of rat mature adipocyte-derived dedifferentiated fat cells as a cell source for periodontal tissue regeneration. Front Physiol 2016;7:50.

[20] Guo L, Ge J, Zhou Y, Wang S, Zhao RCH, Wu Yaojiong. Three-dimensional spheroid-cultured mesenchymal stem cells devoid of embolism attenuate brain stroke injury after intra-arterial injection. Stem Cell Dev 2014;23:978—89.

[21] English K, French A, Wood KJ. Mesenchymal stromal cells: facilitators of successful transplantation? Cell Stem Cell 2010;7:431—42.

[22] Shi Y, Su J, Roberts AI, Shou P, Rabson AB, Ren G. How mesenchymal stem cells interact with tissue immune responses. Trends Immunol 2012;33:136—43.

[23] Bartosh TJ, Ylöstalo JH, Bazhanov N, Kuhlman J, Prockop DJ. Dynamin compaction of human mesenchymal stem/precursor cells into spheres self-activates caspase-dependent IL1 signaling to enhance secretion of modula-tors of inflammation and immunity (PGE2, TSG6, and STC1). Stem Cell 2013;31:2443—56.

[24] Kikuta S, Tanaka N, Kazama T, Kazama M, Kano K, Ryu J, et al. Osteogenic effects of dedifferentiated fat cell transplantation in rabbit models of bone defect and ovariectomy-induced osteoporosis. Tissue Eng 2013;19:1792—802.

[25] Sugawara A, Sato S. Application of dedifferentiated fat cells for periodontal tissue regeneration. Hum Cell 2014;27:12—21.

[26] Nickel J, Mueller TD. Specification of BMP signaling. Cells 2019;8:1579.

[27] Zhou Z, Xie J, Lee D, Liu Y, Jung J, Zhou L, et al. Neogenin regulation of BMP-induced canonical Smad signaling and endochondral bone formation. Dev Cell 2010;19:90—102.

[28] Chen G, Deng C, Li YP. TGF-β and BMP signaling in osteoblast differentiation and bone formation. Int J Biol Sci 2012;8:272—88.

[29] Li Y, Ge C, Franceschi RT. MAP kinase-dependent RUNX2 phosphorylation is necessary for epigenetic modification of chromatin during osteoblast differ-entiation. J Cell Physiol 2017;232:2427—35.

[30] Ge C, Yang Q, Zhao G, Yu H, Kirkwood KL, Franceschi RT. Interactions between extracellular signal-regulated kinase 1/2 and p38 MAP kinase pathways in the control of RUNX2 phosphorylation and transcriptional activity. J Bone Miner Res 2012;27:538—51.

[31] Shimizu K, Ito A, Honda H. Mag-seeding of rat bone marrow stromal cells into porous hydroxyapatite scaffolds for bone tissue engineering. J Biosci Bioeng 2007;104:171—7.

[32] Hamada K, Hirose M, Yamashita T, Ohgushi H. Spatial distribution of miner-alized bone matrix produced by marrow mesenchymal stem cells in self-assembling peptide hydrogel scaffold. J Biomed Mater Res 2008;84:128—36.